Electronic Component of Dislocation Drag in Metals

G. P. HUFFMAN AND N. LOUAT
Edgar C. Bain Laboratory for Fundamental Research, United States Steel Corporation, Research Center, Monroeville, Pennsylvania 15146

(Received 14 June 1968)

The energy dissipation produced by the electric fields and currents associated with a dislocation moving through a metal is calculated from the Boltzmann equation. The applied stress required for steady motion is found to be proportional to the dislocation velocity divided by the electrical resistivity, in good agreement with low-temperature yield- and flow-stress measurements on bcc metals. The forms of the electric fields and currents are derived, and these are found to exhibit Friedel oscillations and to depend in a unique way on the dislocation velocity. The displacement field of a dislocation is believed to be significantly wider and more gradual in an fcc than in a bcc lattice, and this feature can be taken into account either by (1) inserting dislocation widths into the calculation, or (2) assuming perfect electronic screening of the dislocation deformation potential. The stress or drag coefficient obtained from the width calculation shows a very small temperature dependence, while the perfect-screening result is temperature-independent. The problem of a dislocation moving in a magnetic field applied along its length and perpendicular to its direction of motion is also considered. Under suitable conditions, it is found that oscillatory effects of the cyclotron-resonance type may occur in the stress or drag coefficients.

I. INTRODUCTION

THERE is considerable interest in determining the nature of the interaction between conduction electrons and moving dislocations. At low temperatures, this interaction may be the main retarding force on moving dislocations in metals, and we have previously suggested[1] that the energy dissipated by conduction-electron currents could be the origin of the markedly temperature-dependent component of yield and flow stresses observed in bcc metals.[2–7]

We present here an extension of previous work,[1,8] using the Boltzmann equation approach to calculate this energy dissipation. In Sec. II, we present a general formulation of the problem, which is closely analogous to the acoustic attenuation theory of Cohen, Harrison, and Harrison.[9] Section III treats the case of dislocations moving in zero applied field, and gives further details on the results of previous work. In addition, two possible mechanisms which may explain the much smaller temperature dependence of dislocation drag in fcc metals relative to bcc metals are presented. The first method introduces dislocation widths into the calculation. The larger widths appropriate for fcc metals relative to bcc metals reduce the size and temperature dependence of the drag appreciably for the former. The second method assumes that, because dislocations are more spread out in fcc than in bcc lattices, electrons are able to screen almost perfectly the deformation potential in the former. This produces a temperature-independent drag of about the right magnitude. Present experimental results are not sufficient to determine which of these methods (presumably two different approximate descriptions of the same physical mechanism) is nearer the truth. In Sec. IV, the effect of an applied magnetic field is considered and cyclotron-resonance effects are found. For bcc metals, the effect is small, producing a change of perhaps 5% in the stress on drag coefficients under optimum conditions. If the dislocation width concept is used to describe fcc metals, the magnetic effect is found to be comparable in size and form to the bcc case. However, use of the nearly-perfect-screening assumption predicts quite marked oscillations in the stress, having magnitudes of 10–30% of the zero field value. For this and other reasons the magnetic field experiments should be critical in clarifying the problem. The form of the electric fields and currents produced by a moving dislocation is derived in Sec. V, and the possibility of detecting these is discussed. Section VI presents a summary and discussion of the results.

II. BOLTZMANN-EQUATION FORMULATION

Cohen, Harrison, and Harrison have given a general treatment of the problem of ultrasonic attenuation in metals, using a solution of the Boltzmann equation obtained with the trajectory method of Chambers.[10] Using the notation $\mathbf{r}'=\mathbf{r}(t')$, $\mathbf{v}'=\mathbf{v}(t')$, the solution is

$$f(\mathbf{r},\mathbf{v},t)=\int_{-\infty}^{t} f_s(\mathbf{r}',\mathbf{v}',t')e^{-(t-t')/\tau}dt'/\tau. \quad (1)$$

[1] G. P. Huffman and N. P. Louat, Phys. Rev. Letters **19**, 518 (1967); **19**, 774(E) (1967).
[2] H. Conrad and W. Hayes, Trans. Am. Soc. Metals **56**, 125 (1963).
[3] I. M. Bernstein and J. C. M. Li, Phys. Status Solidi **23**, 539 (1967).
[4] J. W. Christian and B. C. Masters, Proc. Roy. Soc. (London) **A281**, 223 (1964).
[5] F. L. Altshuler and J. W. Christain, Phil. Trans. Roy. Soc. (London) **261**, A1121 (1967).
[6] G. A. Beresnev, V. I. Sarrak, and R. I. Entin, Dokl. Akad. Nauk, SSSR **167**, 322 (1966) [English transl.: Soviet Phys.—Doklady **11**, 252 (1966)].
[7] M. J. Marcinkowski and H. A. Lipsitt, Acta Met. **10**, 95 (1962).
[8] N. P. Louat and G. P. Huffman, Bull. Am. Phys. Soc. **13**, 712 (1968).
[9] M. H. Cohen, M. J. Harrison, and W. A. Harrison, Phys. Rev. **117**, 937 (1960), hereafter referred to as CHH.
[10] R. G. Chambers, Proc. Roy. Soc. (London) **A65**, 458 (1962); **A238**, 344 (1957).

Here $f(\mathbf{r},\mathbf{v},t)$ is the electron distribution function, which gives the probability of finding an electron at point $(\mathbf{r},\mathbf{v})$ in phase space at time t; f_s is the distribution function after scattering, and τ is the electronic relaxation time. If $\mathbf{u}(\mathbf{r},t)$ is the velocity imparted to ions and impurities by the moving dislocation, f_s has the form of an ordinary Fermi distribution function centered about velocity $\mathbf{u}$; i.e.,

$$f_s(\mathbf{r},\mathbf{v},t)=f_0(\mathcal{E}(\mathbf{r},\mathbf{v}-\mathbf{u},t)-E_F), \tag{2}$$

where E_F is the Fermi energy and the single-electron energy is given approximately by

$$\mathcal{E}(\mathbf{r},\mathbf{v},t)=\tfrac{1}{2}m\mathbf{v}^2+V_D(\mathbf{r},t)+E_0=\mathcal{E}_0(\mathbf{v})+V_D(\mathbf{r},t). \tag{3}$$

Here, E_0 is the energy at the bottom of the conduction band, and V_D is the deformation potential of the moving dislocation.

The solution to the linearized Boltzmann equation is found by expanding f and f_s to terms which are of first order in $\mathbf{u}$:

$$f(\mathbf{r},\mathbf{v},t)=f_0(\mathcal{E}_0(\mathbf{v})-E_F)+f_1(\mathbf{r},\mathbf{v},t). \tag{4}$$

Following standard procedure,[9,11] one finds

$$f_1(\mathbf{r},\mathbf{v},t)=\left(\frac{-\partial f_0}{\partial\mathcal{E}_0}\right)\int_{-\infty}^{t} e^{-(t-t')/\tau}\{\mathbf{v}'\cdot[e\mathbf{E}(\mathbf{r}',t') -\nabla V_D(\mathbf{r}',t')+m\mathbf{u}(\mathbf{r}',t')/\tau]-V_D(\mathbf{r}',t)/\tau\}, \tag{5}$$

where $\mathbf{E}$ is the electric field produced by the moving dislocation. Following CHH, we Fourier-analyze all quantities and obtain for the electron current

$$\mathbf{J}_e(\mathbf{r},t)=\sum_{\mathbf{q}}\boldsymbol{\sigma}_{\mathbf{q}}\cdot\left\{\mathbf{E}_{\mathbf{q}}+\frac{m\mathbf{u}_{\mathbf{q}}}{e\tau}-\frac{\omega\tau}{(1-i\omega\tau)}\frac{\mathbf{q}V_{D\mathbf{q}}}{e}\right\}e^{i(\mathbf{q}\cdot\mathbf{r}-\omega\tau)}, \tag{6}$$

where the conductivity tensor $\boldsymbol{\sigma}$ is given by

$$\boldsymbol{\sigma}=\int d\mathbf{v}(e\mathbf{v})\mathbf{g}(\mathbf{v})\left(\frac{-\partial f_0}{\partial\mathcal{E}_0}\right), \tag{7}$$

and

$$\mathbf{g}(\mathbf{v})=\int_{-\infty}^{t} e\mathbf{v}'\exp\{i\mathbf{q}\cdot(\mathbf{r}'-\mathbf{r}) -\omega(t'-t)-(t-t')/\tau\}dt'. \tag{8}$$

The requirement of Galilean invariance restricts ω to the values

$$\omega=(\mathbf{q}\cdot\mathbf{b}-2\pi n)/\tau_D, \tag{9}$$

where n is any integer, $\mathbf{b}$ is the Burgers vector, and τ_D is the time required for the dislocation to move from one lattice position to the adjacent position.

All quantities can be expressed in terms of $\mathbf{u}_q$. A simple but reasonable form for the deformation potential is

$$V_{D\mathbf{q}}=-\frac{2E_F}{3}\frac{qu_{q\parallel}}{\omega}\Gamma_q, \tag{10}$$

where $u_{q\parallel}$ is the component of $\mathbf{u}_q$ parallel to $\mathbf{q}$, and Γ_q specifies the screening of the potential by conduction electrons. Following Brown,[12] we adopt the Bardeen or static dielectric screening function,[13]

$$\Gamma_q=\left\{\left(\frac{q}{q_{TF}}\right)^2+\left[\tfrac{1}{2}+\left(\frac{4k_F^2-q^2}{8k_Fq}\right)\ln\left|\frac{2k_F+q}{2k_F-q}\right|\right]\right\}^{-1}, \tag{11}$$

where k_F and q_{TF} are the Fermi and Thomas-Fermi wave vectors, respectively.

Using Maxwell's equations relating the field to the total current, one finds

$$\mathbf{E}_q=(\boldsymbol{\sigma}^{-1}\cdot\mathbf{K}^{-1}\cdot\boldsymbol{\sigma}\cdot\mathbf{A}-\mathbf{1}-\mathbf{V})\cdot(Ne\mathbf{u}_q/\sigma_0) =\mathbf{E}_q\cdot\frac{Ne\mathbf{u}_q}{\sigma_0}, \tag{12}$$

where N is the conduction-electron density, σ_0 is the dc conductivity, and the various tensors are defined by Eqs. (13)–(19).

$$A=(\mathbf{B}^{-1}+\mathbf{1}+\mathbf{V}), \tag{13}$$

$$\mathbf{K}=(\mathbf{1}+\boldsymbol{\sigma}/\sigma_0\cdot\mathbf{B}^{-1}), \tag{14}$$

$$\mathbf{B}^{-1}=(i/\gamma,\ -i/\beta,\ -i/\beta)\ \text{(diagonal)}, \tag{15}$$

$$V_{ij}=0,\ i\neq j\neq 1, \tag{16}$$

$$V_{11}=\rho_q\Gamma_q, \tag{17}$$

where

$$\gamma=\omega/4\pi\sigma_0,\quad \beta=(qc/\omega)^2\gamma, \tag{18}$$

and

$$\rho_q=(q\Lambda)^2/3(1-i\omega\tau), \tag{19}$$

Λ being the electronic mean free path.

Using these results, Eq. (6) can be rewritten in the form

$$\mathbf{J}_{eq}=\mathbf{K}^{-1}\cdot\boldsymbol{\sigma}\cdot\mathbf{A}\cdot Ne\mathbf{u}_q=\mathbf{J}\cdot Ne\mathbf{u}_q. \tag{20}$$

Taking into account collision drag effects,[9,11] the energy dissipated by electrons when the dislocation moves from the jth to the $(j+1)$th lattice position is

$$W=\int_{j\tau_D}^{(j+1)\tau_D}dt\int d^3r\left[\mathbf{J}_e(\mathbf{r},t)\cdot\left(\mathbf{E}(\mathbf{r},t)-\nabla\left\{\frac{V_D(\mathbf{r},t)}{e}\right\}-\frac{m\mathbf{u}(\mathbf{r},t)}{e\tau}\right)+\frac{Nm\mathbf{u}^2(\mathbf{r},t)}{\tau}\right]. \tag{21}$$

Cylindrical symmetry reduces the problem to a two-

[11] H. N. Spector, Solid State Phys. **19**, 291 (1966).

[12] R. A. Brown, Phys. Rev. **141**, 568 (1966).

[13] J. M. Ziman, *Electrons and Phonons* (Oxford University Press, London, 1960), p. 200.

dimensional one, and, Fourier-analyzing, one finds

$$W=-\frac{Nm\tau_D L(\mathrm{cm})^4}{(2\pi)^2\tau}\int d^2\mathbf{q}\,\mathbf{u}_{-\mathbf{q}}\cdot(\mathrm{Re}\mathbf{S}_\mathbf{q})\mathbf{u}_\mathbf{q}\,, \quad (22)$$

where L is the dislocation length and the integration extends over the (1-2) plane in Fig. 1. $\mathbf{S}_\mathbf{q}$ is the dissipation tensor given by

$$\mathbf{S}_\mathbf{q}=\mathbf{J}_\mathbf{q}^{+}\cdot\mathbf{E}_{\mathrm{eff}\mathbf{q}}+1\,, \quad (23)$$

where $\mathbf{J}^+$ is the adjoint of $\mathbf{J}$, and $\mathbf{E}_{\mathrm{eff}}$ is the effective-field tensor,

$$\mathbf{E}_{\mathrm{eff}}=\left\{\boldsymbol{\sigma}^{-1}\cdot\mathbf{K}^{-1}\cdot\boldsymbol{\sigma}\cdot\mathbf{A}-2+\frac{i\mathbf{V}}{\omega\tau}\right\}. \quad (24)$$

We note that the effects of applied fields are included at this stage through their influence on $\boldsymbol{\sigma}$.

III. RESULTS FOR $H=0$

If there are no applied fields, $\boldsymbol{\sigma}$ and the other tensors discussed in Sec. II are diagonal. In particular,[14]

$$\sigma_{11}=\sigma_{\parallel}=\frac{3\sigma_0}{(1-i\omega\tau)a^3}(a-\tan^{-1}a)\,, \quad (25)$$

and

$$\sigma_{22}=\sigma_{33}=\sigma_\perp=\frac{3\sigma_0}{(1-i\omega\tau)2a^3}[(1+a^2)\tan^{-1}a-a], \quad (26)$$

where

$$a=q\Lambda/(1-i\omega\tau). \quad (27)$$

The components of $\mathbf{S}$ in this case are given by

$$\mathbf{S}_{11}=\mathbf{S}_{\parallel}=\frac{\sigma_{\parallel}{}^*v^*}{Q_1{}^*}\left\{\frac{v}{Q_1}-2+\frac{i\rho\Gamma}{\omega\tau}\right\}+1, \quad (28)$$

$$\mathbf{S}_{22}=\mathbf{S}_{33}=\mathbf{S}_\perp=\frac{\sigma_\perp{}^*b^*}{Q_2{}^*}\left\{\frac{b}{Q_2}-2\right\}+1, \quad (29)$$

where

$$v=i/\gamma+\rho\Gamma\,, \quad (30)$$

$$b=(1-i/\beta)\,, \quad (31)$$

$$Q_1=(1+i\sigma_{\parallel}/\gamma)\,, \quad (32)$$

and

$$Q_2=(1-i\sigma_\perp/\beta). \quad (33)$$

The ionic velocity functions are found by taking the time derivative of Eshelby's expressions for the ionic displacement functions of a moving dislocation.[15] One finds, for example, with respect to the $(\hat{\imath},\hat{\jmath},\hat{k})$ system in Fig. 1,

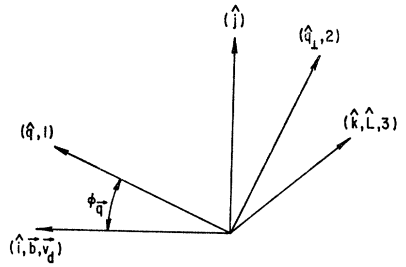

FIG. 1. Calculations in wave-vector space are most easily carried out in the (1,2,3) coordinate system specified by the unit vectors $\hat{q}$, in the direction of $\mathbf{q}$, $\hat{L}$, along the length of the dislocation, and the cross product of these two, $\hat{q}_\perp$. The natural coordinate system in real space $(\hat{\imath},\hat{\jmath},\hat{k})$ is specified by the Burgers vector or glide direction, $\mathbf{b}$, $\hat{L}$, and the direction of their cross product $\hat{\jmath}$.

$$u_x^{(\mathrm{edge})}(x',y)=\frac{bv_d}{2\pi}\left\{\left[2-\left(\frac{v_2}{v_1}\right)^2\right]\frac{y}{(x'^2+y^2)}+\left[2\left(\frac{v_2}{v_1}\right)^2-1\right]\frac{y^3}{(x'^2+y^2)^2}\right\}, \quad (34)$$

where b is the Burgers vector, v_d is the dislocation velocity, v_2 and v_1 are the transverse and longitudinal sound velocity, and

$$x'=x-v_dt. \quad (35)$$

Similar results are found for the other nonvanishing components of interest, $u_y^{(\mathrm{edge})}$ and $u_z^{(\mathrm{screw})}$. The Fourier transforms are readily calculated. Using the (1,2,3) coordinate system of Fig. 1, we find

$$\mathbf{u}_\mathbf{q}^{(\mathrm{edge})}=u_{\mathbf{q}\parallel}{}^{(\mathrm{edge})}\hat{q}+u_{\mathbf{q}\perp}{}^{(\mathrm{edge})}\hat{q}_\perp\,, \quad (36)$$

$$\mathbf{u}_\mathbf{q}^{(\mathrm{screw})}=u_{\mathbf{q}\perp}{}^{(\mathrm{screw})}\hat{L}\,, \quad (37)$$

where

$$u_{\mathbf{q}\parallel}{}^{(\mathrm{edge})}=-i\frac{bv_d}{(\mathrm{cm})^2}\frac{\xi\sin\varphi_\mathbf{q}\cos\varphi_\mathbf{q}}{q}, \quad (38)$$

$$u_{\mathbf{q}\perp}{}^{(\mathrm{edge})}=-i\frac{bv_d}{2(\mathrm{cm})^2}\frac{(1-4\sin^2\varphi_\mathbf{q})}{q}, \quad (39)$$

$$u_{\mathbf{q}\perp}{}^{(\mathrm{screw})}=-i\frac{bv_d}{(\mathrm{cm})^2}\frac{\sin\varphi_\mathbf{q}\cos\varphi_\mathbf{q}}{q}, \quad (40)$$

and

$$\xi=[1+2(v_2/v_1)^2].$$

The cylindrical symmetry has removed any dependence on q_3, and $\omega_\mathbf{q}$ reduces to $qv_d\cos\varphi_\mathbf{q}$ in this continuum approximation.

Introducing a Debye cutoff in the q integration in Eq. (22), one finds that the applied stress required to supply

[14] C. Kittel, *Quantum Theory of Solids* (John Wiley & Sons, Inc., New York, 1963), Chap. 17, p. 236.
[15] J. D. Eshelby, Proc. Phys. Soc. (London) **A62**, 307 (1949).

the energy dissipated by this mechanism is

$$S^{(\text{edge})}=W/b^2L=S_{\parallel}{}^{(\text{edge})}+S_{\perp}{}^{(\text{edge})}$$
$$=\frac{Nmbv_d}{4\pi^2\tau}\left\{\xi^2\int_0^{q_D}dq\int_0^{2\pi}d\varphi\frac{\sin^2\varphi\cos^2\varphi}{q}(\mathrm{Re}\mathbf{S}_{\parallel})\right.$$
$$\left.+\frac{1}{4}\int_0^{q_D}dq\int_0^{2\pi}d\varphi\frac{(1-4\sin^2\varphi)^2}{q}(\mathrm{Re}\mathbf{S}_{\perp})\right\},\quad(41)$$

while

$$S_{\perp}{}^{(\text{screw})}=\frac{Nmbv_d}{4\pi^2\tau}\int_0^{q_D}dq\int_0^{2\pi}d\varphi\frac{\sin^2\varphi\cos^2\varphi}{q}(\mathrm{Re}\mathbf{S}_{\perp}).\quad(42)$$

If one inserts the complete forms for $\mathbf{S}_{\parallel}$ and $\mathbf{S}_{\perp}$, Eqs. (41) and (42) are quite complicated and the integrals can only be done numerically. However, one can convince oneself that the following approximations are valid: (1) $S_{\perp}{}^{(\text{edge})}$ and $S_{\perp}{}^{(\text{screw})}$ are $\ll S_{\parallel}{}^{(\text{edge})}$ over the temperature range of interest (0 to 200 or 300°K); (2) the dominant contribution to the $S_{\parallel}{}^{(\text{edge})}$ integral comes from the region where q is large (i.e., $q\gtrsim q_D/10$). In this high-q region, $q\Lambda\gg1$, and, if we also assume that $\omega\tau\lesssim10^{-1}$, which should be valid for most materials, we find,

$$\mathrm{Re}\mathbf{S}_{\parallel}\approx\left\{\frac{(q\Lambda)^2}{3}(1-\Gamma_q)+\frac{\pi q\Lambda}{6}\right\}\left(1+\frac{q^2}{q_{\mathrm{TF}}{}^2}\Gamma_q\right),\quad(43)$$

where we have neglected terms of order $(\omega\tau)^2$ with respect to 1, and terms of order 1 with respect to $q\Lambda$. Following Pines[16] and others,[17] we replace q_{TF} by a somewhat smaller screening vector, $q_s=0.433\,q_{\mathrm{TF}}$, and adopt the approximation

$$\Gamma_q\approx\frac{1}{(1+q^2/q_s{}^2)}.\quad(44)$$

One then finds, from Eq. (41) (dropping the labels on S),

$$S\cong\frac{Nmbv_d\xi^2}{16\pi\tau}\left\{\frac{(q_D\Lambda)^2}{3}\mathfrak{F}(x_m)+\frac{\pi(q_D\Lambda)}{6}\mathfrak{S}(x_m)\right\},\quad(45)$$

where $x_m=(q_D/q_s)$, and

$$\mathfrak{F}(x_m)=\left\{1+\frac{1}{2(1+x_m{}^2)}-\frac{3}{2x_m{}^2}\ln(1+x_m{}^2)\right\},\quad(46)$$

$$\mathfrak{S}(x_m)=(2-\tan^{-1}x_m/x_m).\quad(47)$$

Both $\mathfrak{F}$ and $\mathfrak{S}$ are typically ~1, so that the second term of (45) may be neglected and the equation rewritten as

$$S\approx\frac{mE_Fbq_D{}^2\xi^2\mathfrak{F}(x_m)}{24\pi e^2}\frac{v_d}{\rho}=C\frac{v_d}{\rho},\quad(48)$$

where ρ is the dc electrical resistivity. The electron drag coefficient, measured in ultrasonic or internal friction experiments, is simply given by $B=(Cb/\rho)$. If we neglect other dislocation drag mechanisms, we can equate S to the yield stress. More accurately, we mean the flow stress extrapolated back to the elastic line on the stress-strain curve.[5] The term "yield stress" is used because it represents a fairly well-defined point on this curve, at which interactions between dislocations (work-hardening) should be negligible. For measurements at constant strain rate, as discussed previously,[1] v_d can be assumed to be approximately independent of temperature, so that all of the temperature dependence is contained in ρ. Separating ρ into its ideal and residual parts, and inverting Eq. (48), we find

$$\frac{1}{S}=\frac{1}{C}\frac{(\rho_i(T)+\rho_0)}{v_d}.\quad(49)$$

A plot of $1/S$ versus ρ_i should then give a straight line whose slope and intercept determine the dislocation

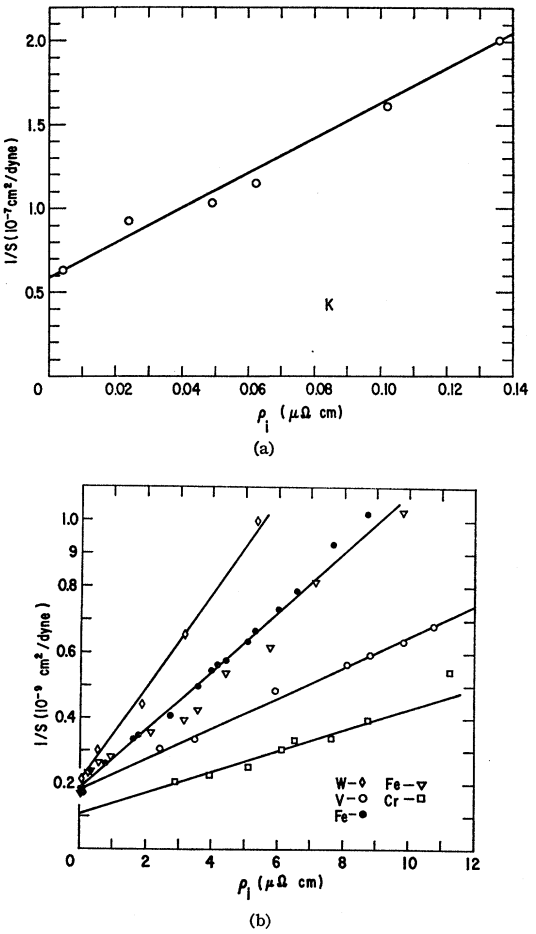

FIG. 2. The inverse yield stress versus the ideal resistivity for (a) K (Ref. 3); (b) Fe (Refs. 5 and 6), Cr (Ref. 7), V (Ref. 4), and W (Ref. 4).

[16] D. Pines, Solid State Phys. 1, 367 (1955).
[17] K. Krebs, Phys. Rev. 138, A143 (1965).

velocity and the residual resistivity of the specimen, respectively. Several examples are shown in Fig. 2, and the dislocation velocities and residual resistivities found from these and other such plots are listed in Table I. If one now takes these values and uses them in Eq. (48), one finds the theoretical S-versus-T dependence shown by the smooth curves in Fig. 3.

It may be noted that theory and experiment are in better accord at low than at high temperatures. This is expected since other dislocation drag mechanisms (phonon drag, impurity and grain boundary pinning, etc.) should become comparable to or greater than the electronic component at higher temperatures. If one could subtract the part of the dislocation drag due to these mechanisms, the straight-line relationship would presumably hold for the electronic component at elevated temperatures, but since there is no standard procedure for doing this we have not attempted it.

Reference to the table shows that the dislocation velocities obtained are fairly large, being about 10% of the speed of sound in most cases. These values contrast with those obtained from etch-pit experiments, namely,

TABLE I. Dislocation velocities and residual resistivities for various bcc metals.

Element	v_d(cm/sec)	$\rho_0(\mu\Omega$ cm)
V	5.88×10^4	3.88
Fe	2.18×10^4	2.06
Cr	6.22×10^4	3.35
W	1.89×10^4	1.39
Mo	2.27×10^4	2.17
Nb	7.83×10^4	5.06
Ta	6.64×10^4	3.85
K	11.86	0.054

$\sim10^{-2}$ cm/sec or less. However, this discrepancy may be more apparent than real, since this experimental approach gives only an average velocity over a large distance, ~1 mm, and affords no information on how long or how often the dislocation may have stopped. We are concerned here with the primary velocity with which a dislocation moves between neighboring lattice positions separated by one Burgers vector. The speed of this motion should be determined by the strength of the atomic bonding, just as is the speed of sound-wave propagation, and, on this basis, velocities several percent of the speed of sound seem quite realistic. Moreover, several recent experiments are in qualitative agreement with our results.[18]

We note that, although the residual resistivities are of reasonable size, they are, in general, somewhat higher

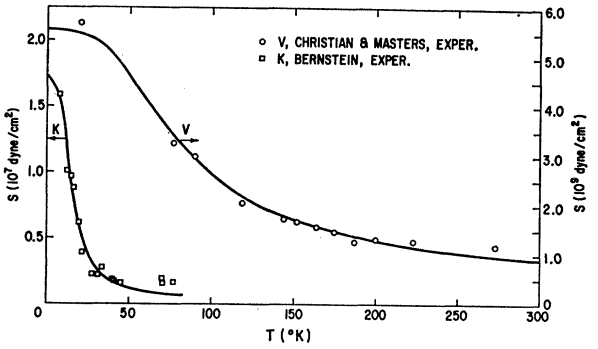

(a)

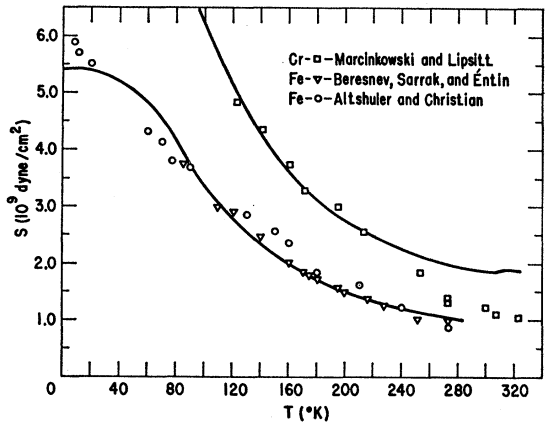

(b)

FIG. 3. Theoretical (smooth curves) and experimental (points) yield stress versus temperature results for (a) K (Ref. 3) and V (Ref. 4); (b) Fe (Refs. 5 and 6) and Cr (Ref. 7).

than one might have expected on the basis of specimen purity. Further, the same residual resistance seems to be appropriate for the Fe data of two different investigators. This was also found to be approximately true for other metals, where more than one set of data was available. These facts suggest that the residual resistance in this theory should be viewed as a parameter which is characteristic of the electronic mean free path in the highly strained region close to the dislocation core. This seems reasonable, since the dominant part of the interaction takes place for large q, $\gtrsim q_D/10$, so that most of the energy dissipation takes place within a distance of several Burgers vectors from the dislocation center.

For $\omega\tau>10^{-1}$, the approximate expressions (43) and (48) are no longer accurate, and one must consider the more complicated complete expressions for $S_{\parallel}$ and $S_{\perp}$. Thus, for example,

$$\mathrm{Re}\mathbf{S}_{\parallel}=\frac{(q\Lambda)^2}{3[1+(\omega\tau)^2]}\times\left\{\mathfrak{L}+\frac{[x^2\omega\tau(\Sigma_I-x^2\omega\tau)\mathfrak{L}+\Sigma_R\mathfrak{K}]}{[\Sigma_R{}^2+(\Sigma_I-x^2\omega\tau)^2]}\right\}, \quad (50)$$

[18] R. M. Fisher and J. S. Lally, Can. J. Phys. 45, 1147 (1967); K. Marukawa, Institute for Solid State Physics, University of Tokyo, Technical Report No. 222, 1966, Sec. A (unpublished); F. Vreeland, Jr., in *Dislocation Dynamics*, edited by A. R. Rosenfield, G. L. Hahn, A. L. Bement, and R. I. Jaffee (McGraw-Hill Book Co., New York, 1968), p. 529.

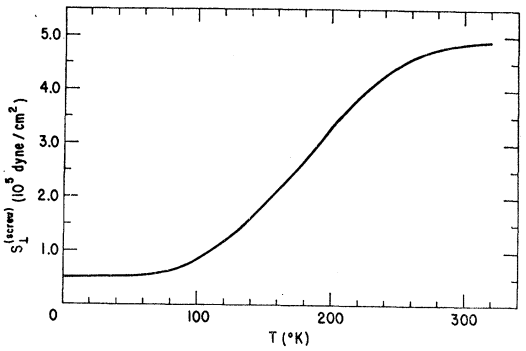

FIG. 4. Stress versus temperature for a screw dislocation in a typical free-electron metal assuming a conduction-electron density of 5×10^{22} cm^{-3} and a dislocation velocity of 10^4 cm/sec. $S_\perp^{(edge)}$ has a very similar form.

where $x=q/q_s$, $\omega=qv_d\cos\varphi$, and

$$\mathfrak{L}=-\Gamma(1+x^2\Gamma)-\frac{6}{(q\Lambda)^2}\{1+(\omega\tau)^2(1+x^2\Gamma)\}, \quad (51)$$

$$\mathfrak{IC}=(1+x^2\Gamma)[1+(\omega\tau)^2(1+x^2\Gamma)]-\frac{6}{(q\Lambda)^2}x^4(\omega\tau)^2\Gamma, \quad (52)$$

$$\Sigma_R=\frac{(q\Lambda)^2}{3}\,\mathrm{Re}\sigma_{11}, \quad \Sigma_I=\frac{(q\Lambda)^2}{3}\,\mathrm{Im}\sigma_{11}. \quad (53)$$

We have evaluated (41) and (42) by computer integration, using the complete expressions for $\mathbf{S}_{11}$, $\mathbf{S}_\perp$ and the complete screening function Γ as given by Eq. (11). These calculations confirm that $S_\perp \ll S_{11}$ over the temperature range of interest. The transverse component of drag is found to increase with increasing temperature, and this is shown in Fig. 4 for a screw dislocation in a typical metal. The relatively small magnitude of the stress arises primarily because the displacement field we have assumed for a moving screw dislocation has no dilation. If, in fact, this is not the case, this result could be greatly altered.

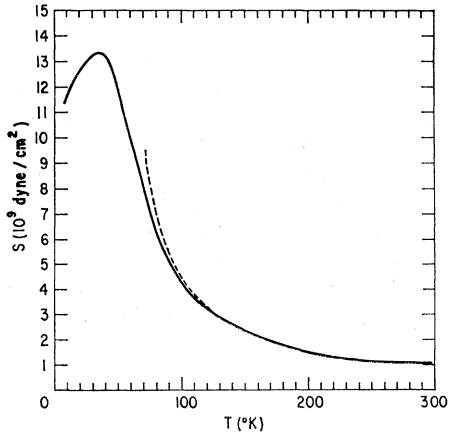

FIG. 5. Results of computer integration of the complete expression [Eq. (50)] for S_{11} (solid line) and the approximate results given by Eq. (48) for V parameters (dashed line), but assuming a residual resistance parameter of 0.16 $\mu\Omega$ cm. For this example, $\omega_m\tau\sim10^{-1}$ at $T=100$°K, and $\omega_m\tau\sim1$ at $T=40$°K.

The numerical integration result for S_{11} is shown in Fig. 5. Here, we have used the parameters of V, but have assumed $\rho_0=0.16$ $\mu\Omega$ cm in order to obtain values of $\omega_m\tau>1$, where ω_m is the maximum frequency associated with the dislocation wave packet $q_D v_d$. The dashed line is the approximate result of Eq. (48) using the same parameters. The agreement is seen to be rather good for $\omega\tau<10^{-1}$. For $\omega\tau>1$, S_{11} passes through a maximum and subsequently decreases. To our knowledge, such a maximum has not been observed experimentally in either yield-stress or damping experiments. However, a leveling off of the yield stress at low temperatures, which is predicted even by the approximate form of the theory, has been observed in both Fe [5] and K.[19] Whether or not a maximum is observable would depend to a large extent on the value of the residual resistance parameter ρ_0, since, as discussed above, this is larger (and the effective relaxation time correspondingly smaller) than the value corresponding to sample purity. The example given here is, of course, purely hypothetical, since $\rho_0=3.88$ $\mu\Omega$ cm in V, and we include it only to call attention to the possibility of such an effect in other materials.

The yield- and flow-stress data for fcc[20,21] and hexagonal metal[22] show a very small temperature dependence compared to bcc metals. In addition, ultrasonic experiments on fcc metals show a damping coefficient which is insensitive to temperature.[23,24] One possible explanation of these results is found by introducing dislocation widths into the calculation. In the usual manner,[25] we define λ as the half-width of the dislocation. It is believed that the core distortion is spread out over a considerably larger region in fcc than in bcc lattices, and reasonable width estimates are $\lambda\approx\frac{1}{4}b$ for bcc, and $\lambda\approx1$ or $2b$ for fcc metals. The only change in the theory occurs in the ionic velocity function. For example, in Eq. (34), one replaces y by $(y+\lambda)$ everywhere. The Fourier transforms are still easily calculated, and one finds

$$u_{\mathbf{q}}^{(edge)}=-\frac{i}{\mathrm{cm}^2}(bv_d)\xi e^{-q\lambda\cos\varphi_q}\,\frac{\cos\varphi_q\sin\varphi_q}{q}, \quad (54)$$

with similar changes in the other components. The

[19] D. Hull and H. M. Rosenberg, in *Proceedings of the Tenth International Congress of Refrigeration, Copenhagen, 1959*, edited by A. Mae and M. Jul (Pergamon Press, Inc., New York, 1960), Vol. 1, p. 58.
[20] O. Vohringer and E. Macherauch, Phys. Status Solidi **19**, 793 (1967).
[21] A. S. Keh and Y. Nakada (private communication).
[22] R. N. Orava, G. Stone, and H. Conrad, Trans. Am. Soc. Metals **59**, 171 (1966).
[23] A. Hikata and C. Elbaum, Phys. Rev. Letters **18**, 750 (1967).
[24] B. R. Tittmann and H. E. Bommel, Phys. Rev. **151**, 178 (1966).
[25] R. E. Peierls, Proc. Phys. Soc. (London) **52**, 23 (1940).

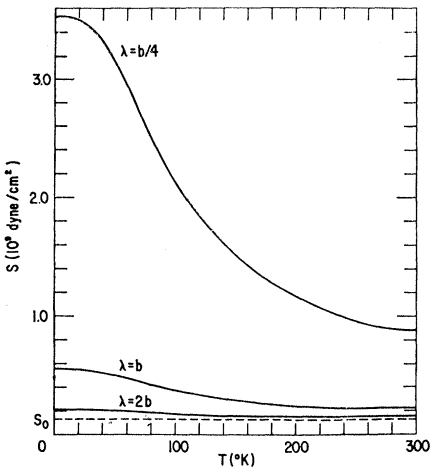

FIG. 6. Stress-versus-temperature results for dislocations of various widths in Cu, assuming $v_d = 10^4$ cm/sec.

S-versus-T curves resulting from a computer integration for S_{11} are shown in Fig. 6, using parameters which should be reasonable for Cu. We assume that the total stress is the electronic component plus a constant term S_0, indicated by the dotted line, which has been estimated from yield-stress data for pure Cu.[20] The S-versus-T curves are seen to depend markedly on the width parameter, the results being quite similar to the bcc case for $\lambda = \frac{1}{4}b$, while the temperature dependence is extremely small for $\lambda = 2b$. It is found that the electronic component of S can be approximately represented by the expression

$$S(\lambda) \approx \exp(-q_D \lambda \alpha)(C v_d/\rho), \tag{55}$$

where α is a parameter which depends on λ, but is generally of order 1. We note that the temperature dependence could be even smaller, if one considered the nonelectronic component to be increasing with temperature, as might be appropriate for phonon drag.[26]

However, a number of experimental results indicate that an alternative explanation may be more suitable for the fcc case. It is found that adding small percentages of impurities to fcc metals markedly increases the yield- and flow-stress temperature dependence,[20,21] suggesting that, even in very pure fcc metals, the small temperature dependence observed may be impurity-controlled. For bcc metals, the main effect of adding impurities is to add a constant term to the stress, while the temperature dependence is not greatly affected,[27] suggesting that any temperature dependence associated with impurities is small compared to that already present in the pure metal. As mentioned previously, ultrasonic experiments, in which dislocations are vibrated between pinning points, show a damping coefficient which is relatively insensitive to temperature.[23,24] Presumably, the only dislocation drag mechanism operative in this experiment, other than the electronic component, is that due to phonons, which should be small at these temperatures.

A dislocation in fcc lattice corresponds to a situation in which atoms are deviated by relatively small amounts from their normal positions over a large region of the crystal, at least in comparison to the bcc case. Because of this, one is led to postulate that the electrons may be able to screen the deformation potential almost perfectly. This approximation is inserted by putting $\Gamma_q \approx 1$, and it is clear from Eq. (43) that the temperature-sensitive part of the stress then vanishes, and that one finds the temperature-independent result

$$S_{11}^{(\text{edge})} \approx \frac{N m b v_d v_F q_D \xi^2}{96}. \tag{56}$$

This is $\sim 10^7$(dyn/cm^2) for a typical metal, and the $S_\perp$ components are again negligible. The drag coefficient in this case is $B = (N m b^2 v_F q_D \xi^2/96)$.

The existing experimental data for fcc metals can probably be explained equally well by either approach. Indeed, it seems likely that, in some improved theory, the two approaches might appear as two different approximate descriptions of the same phenomenon, since the basic effect of each is to emphasize the contribution of somewhat longer-wavelength components of the Fourier synthesis. However, as will be discussed in the next section, the energy dissipation of moving dislocations in an applied magnetic field depends markedly on the amount of screening. Such experiments should therefore be able to establish which approximation is closer to the truth.

IV. ELECTRON DRAG IN AN APPLIED MAGNETIC FIELD

We consider only the simplest situation, that of an applied field H directed along the length of the dislocation (axis 3 in Fig. 1). The conductivity tensor, and thus the tensors $\mathbf{K}$ and $\mathbf{S}$, are no longer diagonal. Equations (4.1) and (4.2) of CHH give the complete expressions for $\boldsymbol{\sigma}$ for this geometry ($\mathbf{q} \perp \mathbf{H}$). As for the zero-applied-field case, the dominant contribution to the integrals in (41) comes from the high q region, $q \gtrsim q_{D/10}$. In this region $\mathbf{S}_{11}$ is much greater than either the transverse ($\mathbf{S}_{22}$ and $\mathbf{S}_{33}$) or off-diagonal components ($\mathbf{S}_{12}$ and $\mathbf{S}_{21}$) of $\mathbf{S}$, and to a good approximation has the same form as given by Eq. (28). Using the same large-q approximations as CHH for σ_{11}, it can be shown that

$$\mathrm{Re}\mathbf{S}_{11} \approx \frac{(q\Lambda)^2}{3} \frac{\{(\Sigma_R - |\Sigma|^2\Gamma)(1+x^2\Gamma) + \Sigma_I \omega\tau(1+x^2\Gamma)^2\}}{\{[1+(\omega\tau)^2]|\Sigma|^2 + 2x^2[\Sigma_R(\omega\tau)^2 - \Sigma_I\omega\tau] + x^4(\omega\tau)^2\}}, \tag{57}$$

[26] W. P. Mason, Phys. Rev. **143**, 229 (1965).
[27] A. S. Keh and Y. Nakada, Can. J. Phys. **45**, 1101 (1967).

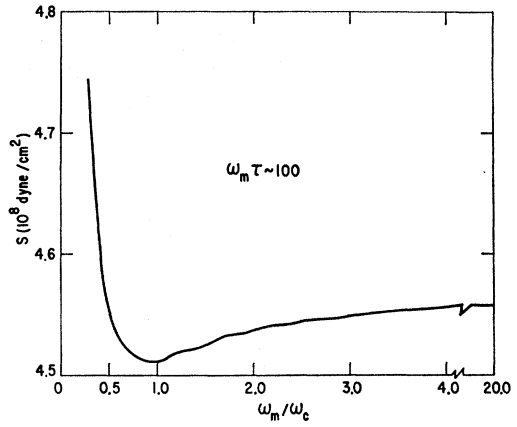

FIG. 7. Stress versus ω_m/ω_c for a bcc metal.

where Σ_R and Σ_I are the real and imaginary parts of

$$\Sigma = 1-(\pi/2a)\coth Z, \tag{58}$$

with

$$Z=(\pi/\omega_c\tau)(1-i\omega\tau), \tag{59}$$

ω_c being the cyclotron frequency (eH/mc). The magnitude of the effect depends sensitively on the size of $\omega\tau$ relative to $q\Lambda$. For $v_d\sim 10^4$ cm/sec, $\omega\tau$ values as large as 10 to 100 are possible. Numerical integration of the first term of Eq. (41) using Eq. (57) gives the results of the type shown in Fig. 7, where we have plotted the stress at constant temperature against the ratio ω_m/ω, ω_m being the maximum frequency associated with the dislocation wave packet, $q_D v_d$. The curve corresponds to the parameters of V, but assumes a large relaxation time $\tau=10^{-11}$ sec. As discussed in Sec. III, it is unlikely that such large "effective" relaxation times could be attained, and since the total change in yield stress or drag coefficients is only ~ 3 or 4%, even for this optimum case, it is doubtful whether the behavior of Fig. 7 could be observed in any detail. One might hope, however, that at least the general shape of the curve, showing a small decrease from the $H=0$ case to a minimum in the vicinity of $\omega_m/\omega_c\sim 1$, and a subsequent sharp rise, might be experimentally observable. A measurement of the value of ω_c at which the minimum occurs would constitute a direct measurement of the dislocation velocity.

If one uses the approximation of nearly-perfect screening for fcc metals discussed in the previous section, the magnetic-field behavior is quite striking. One finds, for the dissipation tensor,

$$\mathrm{Re}\mathbf{S}_{11}\approx\frac{\pi q\Lambda}{6}\frac{\{\mathrm{Re}[(1-i\omega\tau)\coth Z](1+x^2)-\omega\tau\,\mathrm{Im}[(1-i\omega\tau)\coth Z](1+x^2)^2\}}{[1+(\omega\tau)^2(1+x^2)^2]}. \tag{60}$$

Inserting this result into Eq. (41) and performing a computer integration, one finds the results shown in Fig. 8, using parameters appropriate for Cu. The oscillations are much more dramatic, being about 10–30% of the zero field stress. Again, because of the somewhat large residual resistivities associated with the region near the dislocation core, there might be an inherent difficulty in obtaining $\omega_m\tau$ values even as large as 10. Nevertheless, this problem should be much less severe for fcc than for bcc metals, and it seems likely that some oscillatory behavior should be observable if the perfect-screening approximation is the most valid approach for the fcc lattice. The locations and separations of such oscillations could be used to determine, among other things, the primary velocity of a dislocation moving between adjacent lattice positions.

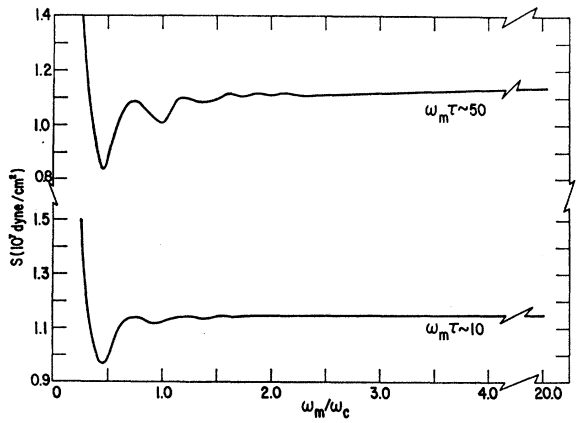

FIG. 8. Stress versus ω_m/ω_c for Cu parameters ($v_d=10^4$ cm/sec) assuming perfect screening.

For the purpose of comparison, we show in Fig. 9 the results for Cu parameters obtained when the perfect-screening approximation is not made. The bottom curve results from treating Cu as if it were a bcc metal, i.e., inserting (57) into (41), while the top curve is found by using (57) for $\mathrm{Re}\mathbf{S}_{11}$ and, in addition, inserting a width of $\lambda=2b$ into the ionic velocity function as in Eq. (54). It is clear that the use of dislocation widths produces a magnetic-field behavior much closer to the bcc results than does the perfect-screening assumption. Such experiments should therefore clearly establish which description of the fcc dislocation is most valid.

We note also that these effects are somewhat enhanced by going to lower electron densities, while the required magnetic fields ($\sim 10^4$–10^5 G) are reduced if the effective electron mass is small. It might be of interest, therefore, to examine a semimetal, such as Bi, even though the calculations given here do not pertain to that situation.

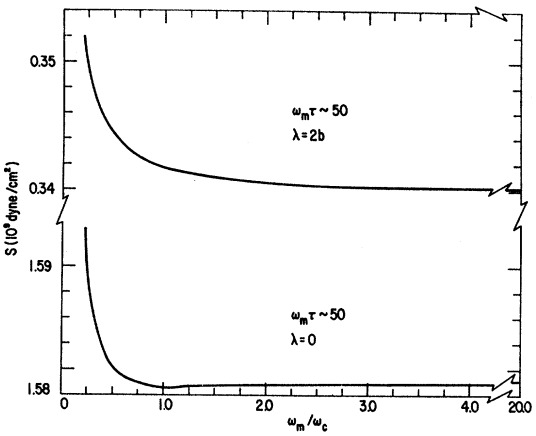

FIG. 9. Stress versus ω_m/ω_c for Cu parameters. The bottom curve makes no allowance for dislocation width, treating Cu in the same manner as bcc metals. The calculation of the top curve differs from that of the bottom through the insertion of a width $\lambda=2b$ into the ionic velocity function.

V. ELECTRIC FIELDS AND CURRENTS

It is of interst to consider the forms of the electric fields and currents in coordinate space. One has only to retransform Eqs. (12), (20) and (24). Making the same approximations discussed in Sec. III, we assume that the dominant contribuiton comes from large q values and neglect terms $\sim(\omega\tau)^2$. For the zero-applied-field case, one finds

$$\mathbf{E}_{l\mathbf{q}}\approx\tfrac{1}{3}(q\Lambda)^2(1-\Gamma_q)\{1+i\omega\tau(1-\Gamma_q)(1+x^2)\}, \quad (61)$$

$$\mathbf{E}_{l\mathrm{eff}\mathbf{q}}\approx\tfrac{1}{3}(q\Lambda)^2\{(1-\Gamma_q)+i[\Gamma_q/\omega\tau+\omega\tau(1-\Gamma)(1+x^2)]\}, \quad (62)$$

$$\mathbf{J}_{el\mathbf{q}}\approx 1-(\omega\tau)^2x^2(1+x^2)(1-\Gamma_q)+i\omega\tau x^2(1-\Gamma_q), \quad (63)$$

where $x=(q/q_{\mathrm{TF}})$. Again the transverse components are found to be small with respect to the longitudinal ones and we neglect them. The retention of the $(\omega\tau)^2$ term in $\mathbf{J}_{el}$ is necessary in order to satisfy Maxwell's equations.

One must now calculate integrals of the form

$$\mathbf{E}(\mathbf{r}')=\frac{\mathrm{cm}^2}{(2\pi)^2}\frac{N_e}{\sigma_0}\int d^2\mathbf{q}\,\exp(i\mathbf{q}\cdot\mathbf{r}')\hat{q}\mathbf{E}_{l\mathbf{q}}u_{l\mathbf{q}}, \quad (64)$$

where $\mathbf{r}'=\hat{\imath}(x-v_dt)+\hat{\jmath}y$. Inserting (61) and (38), one finds

$$\mathbf{E}(\mathbf{r}')=\frac{Nev_db\xi}{(2\pi)^2\sigma_0}\frac{(\Lambda)^2}{3}(\mathbf{I}_1+\mathbf{I}_2), \quad (65)$$

where

$$\mathbf{I}_1=\int_0^\infty qdq\int_0^{2\pi}d\varphi\,e^{iq(x'\cos\varphi_q+y\sin\varphi_q)}q^2(1-\Gamma_q)(-i)\times\{\hat{\imath}(\cos^2\varphi_q\sin\varphi_q/q)+\hat{\jmath}(\cos\varphi_q\sin^2\varphi_q/q)\}, \quad (66)$$

and $\mathbf{I}_2$ has a similar form. This can be rewritten as

$$\mathbf{I}_1=-\frac{\partial}{\partial x'}\nabla'\int_0^\infty dq\times\int_0^{2\pi}d\varphi\,e^{iq(x'\cos\varphi+y\sin\varphi)}(-i)(1-\Gamma_q)\sin\varphi. \quad (67)$$

Performing the φ integration, one finds

$$\mathbf{I}_1=-\frac{\partial}{\partial x'}\nabla'\int_0^\infty dq(1-\Gamma_q)J_1(qr'). \quad (68)$$

This integral has been treated by Brown[12] in the calculation of the deformation potential of a stationary edge dislocation. The result is

$$\mathbf{I}_1=\frac{\partial}{\partial x'}\nabla'\left(\frac{2k_FC_0\sin(2k_Fr'+\frac{1}{4}\pi)}{(2k_Fr')^{5/2}}\right), \quad (69)$$

neglecting terms smaller than those of order $(2k_Fr')^{-5/2}$. Here k_F is the Fermi wave vector, and C_0 is a dimensionless constant,

$$C_0=[(2\pi)^{1/2}\pi(k_Fa_0)^2(1+1/2\pi k_Fa_0)^2]^{-1}, \quad (70)$$

a_0 being the first Bohr radius h^2/me^2. Brown has shown that this approximate answer is quite accurate for $|\mathbf{r}'|\gtrsim b$.

All of the pertinent integrals can be done in a similar fashion, and one finds the following results:

$$\mathbf{E}(\mathbf{r}')=-\frac{4\pi Nb\xi E_FC_0}{k_{Fe}}\hat{r}'\sin\varphi\left[(2k_Fv_d\tau)\cos\varphi\frac{\sin(r_F'+\frac{1}{4}\pi)}{r_F'^{5/2}}+(2k_Fv_d\tau)^2\cos^2\varphi\left(\frac{4k_F^2+q_{TF}^2}{q_{TF}^2}\right)\frac{\cos(r_F'+\frac{1}{4}\pi)}{r_F'^{5/2}}\right], \quad (71)$$

$$\mathbf{E}_{\mathrm{eff}}(\mathbf{r}')=\mathbf{E}+\frac{4\pi Nb\xi E_FC_0}{k_Fe}\left\{\left[-\hat{\imath}\frac{2\cos\varphi\sin\varphi}{(r_F')^2}+\hat{\jmath}\frac{(1-2\sin^2\varphi)}{(r_F')^2}\right]+\hat{r}'\sin\varphi\frac{\cos(r_F'+\frac{1}{4}\pi)}{(r_F')^{5/2}}\right\}, \quad (72)$$

$$\mathbf{J}_e(\mathbf{r}')=Nev_d\left(\frac{k_Fb\xi}{2\pi}\right)\left\{\frac{(\sin^2\varphi-\cos^2\varphi)}{r_F'}(\hat{\imath}\sin\varphi-\hat{\jmath}\cos\varphi)+\hat{r}'(2k_Fv_d\tau)\left(\frac{8k_F^2}{q_{TF}^2}\right)\cos^2\varphi\sin\varphi\left[-\frac{\cos(r'_F+\frac{1}{4}\pi)}{(r_F')^{5/2}}+(2k_Fv_d\tau)\left(\frac{4k_F^2+q_{TF}^2}{q_{TF}^2}\right)\frac{\cos\varphi\sin(r_F'+\frac{1}{4}\pi)}{(r_F')^{5/2}}\right]\right\}, \quad (73)$$

where $\hat{r}'$ is a unit vector in the direction of $\mathbf{r}'$, $r_F'=2k_F|\mathbf{r}'|$, and φ is the angle between $\mathbf{r}'$ and $\mathbf{b}$. These results are appropriate for an edge dislocation moving in a bcc metal. It is revealing to rewrite the effective electric field in the form

$$\mathbf{E}_{\rm eff}(\mathbf{r}')=\mathbf{E}-\nabla'\left(\frac{V_{\rm def}(\mathbf{r}')}{e}\right), \tag{74}$$

where the deformation potential for the moving dislocation is given by

$$V_{\rm def}(\mathbf{r}')=\frac{2E_F}{3}\left(\frac{b\xi}{2\pi}\right)\left[\sin\varphi\left(\frac{1}{r'}+2k_FC_0\frac{\sin(2k_Fr'+\frac{1}{4}\pi)}{(2k_Fr')^{5/2}}\right)\right]. \tag{75}$$

We note also that the total current associated with the moving dislocation is given by

$$\mathbf{J}_{\rm tot}(\mathbf{r}')=\mathbf{J}_e(\mathbf{r}')-Ne\mathbf{u}(\mathbf{r}')=Nev_d\left(\frac{k_Fb}{2\pi}\right)\left\{\left[\hat{\imath}\left(\frac{4\sin^3\varphi}{r_F'}-\frac{5\sin\varphi}{r_F'}\right)+\hat{\jmath}\left(\frac{4\cos^3\varphi}{r_F'}-\frac{3\cos\varphi}{r_F'}\right)\right]\right.$$
$$\left.+\hat{r}'(2k_Fv_d\tau)\left(\frac{8k_F^2}{q_{TF}^2}\right)\cos^2\varphi\sin\varphi\left[-\frac{\cos(r_F'+\frac{1}{4}\pi)}{(r_F')^{5/2}}+(2k_Fv_d\tau)\left(\frac{4k_F^2+q_{TF}^2}{q_{TF}^2}\right)\cos\varphi\frac{\sin(r_F'+\frac{1}{4}\pi)}{(r_F')^{5/2}}\right]\right\}. \tag{76}$$

The consistency of the results is verified by showing that the relation

$$\nabla\cdot\dot{\mathbf{E}}=-4\pi\nabla\cdot\mathbf{J}_{\rm tot}, \tag{77}$$

obtained from Maxwell's equations and the continuity equation, is satisfied.

The total charge density is obtained from the divergence of $\mathbf{E}_{\rm eff}$. One finds,

$$\rho(\mathbf{r}')=-Ne\left(\frac{k_Fb\xi}{2\pi}\right)(2\pi k_Fa_0C_0)\left[\frac{\sin\varphi\sin(r_F'+\frac{1}{4}\pi)}{(r_F')^{5/2}}\right.$$
$$\left.+(2k_Fv_d\tau)\cos\varphi\sin\varphi\frac{\cos(r_F'+\frac{1}{4}\pi)}{(r_F')^{5/2}}-(2k_Fv_d\tau)^2\cos^2\varphi\frac{(4k_F^2+q_{TF}^2)}{q_{TF}^2}\frac{\sin\varphi\sin(r_F'+\frac{1}{4}\pi)}{(r_F')^{5/2}}\right]. \tag{78}$$

For $v_d=0$, this result reduces to that of Brown for a stationary edge dislocation, as required. We note that the Maxwell field $\mathbf{E}$, given by Eq. (71), does not give the correct microscopic charge density, since it does not contain the important deformation-potential term. One could now insert this charge density into an integral involving the Sternheimer antishielding factor to obtain the electric field gradient using the same methods that have previously been used for impurity atoms and stationary dislocations.[28,29] Such electric field gradients are known to produce sizable NMR line-broadening for stationary dislocations.[30,31] For a moving dislocation, therefore, there should be additional broadening, comparable in magnitude, proportional to $(2k_Fv_d\tau)$ and $(2k_Fv_d\tau)^2$. Observation of this effect, however, would require that the mobile dislocation density be comparable to the total dislocation density, and, if the high dislocation velocities obtained in this work are indeed correct, very high strain rates would be required to attain this condition.[1]

It is also possible that the true electric field and total current, given by Eqs. (71) and (76) might be detectable. The electric field oscillates at a frequency of $2k_Fv_d$, about 10^{12} cps, and is quite sizable, having magnitudes of about 8×10^2, 2.6, and 8×10^{-3} statV/cm at $|\mathbf{r}'|=b$, $10b$, and $100b$, respectively. The first, nonoscillatory term in the total current density has zero divergence, and would produce no net current through any closed surface surrounding the dislocation. The second, oscillatory term has the same frequency as the electric field, 10^{12} cps, and has magnitudes of about 10^{13}, 10^{10}, and 10^7 statA/cm^2 at $|\mathbf{r}'|=b$, $10b$, and $100b$. For the electromagnetic effects of these fields and currents to be observed by detectors external to the yielding specimen, the dislocations would have to be within the skin depth distance from the surface, which would be about 10^{-6}–10^{-5} cm for these frequencies, so that boundary conditions would no doubt alter the nature of the signal considerably from what one would expect on the basis of the simple results of Eqs. (71) and (76). Nevertheless, any measurement which could determine even qualita-

[28] W. Kohn and S. H. Vosko, Phys. Rev. **119**, 912 (1960).
[29] T. O. Ogurtani and R. A. Huggins, Phys. Status Solidi **24**, 301 (1967).
[30] E. A. Faulkner, Phil. Mag. **5**, 843 (1960).
[31] T. O. Ogurtani and R. A. Huggins, Phys. Rev. **137**, A1736 (1965).

tively the frequency and intensity of such fields could be processed to yield values for two previously undetermined quantities of great importance: the primary dislocation velocity and the mobile dislocation density.

VI. SUMMARY AND DISCUSSION

The applied stress required to do work at a rate equal to the energy dissipation of the effective electric field and conduction-electron currents associated with a moving dislocation in a metal has been shown to be proportional to the dislocation velocity divided by the electrical resistivity. This result is in good agreement with yield- and flow-stress measurements on bcc metals at low temperatures. Two possible formulations of the problem of a dislocation moving in a fcc lattice have been given. One of these makes use of the concept of dislocation widths. It is found that the larger width parameter appropriate for fcc materials markedly reduces the electronic component of drag, and thus the temperature dependence of the total dislocation drag, with respect to the bcc case. The second approach also makes use of the idea that a dislocation is wider in a fcc than in a bcc lattice, but inserts the concept into the calculation from a different viewpoint, by assuming that, because of this, electrons are able to screen the deformation potential almost perfectly. A temperature-independent stress or damping coefficient is obtained by this method, in agreement with the result of a simple scattering calculation by Holstein,[24] who also assumed a screening function $\Gamma_q=1$.

Application of a magnetic field along the length of the dislocation, perpendicular to the direction of motion is found to produce effects analogous to cyclotron-resonance phenomena in acoustic experiments. For bcc metals, the effect is small, producing only very slight oscillatory behavior in stress versus ω_m/ω_c curves, with a minimum near $\omega_m/\omega_c=1$, which is expected to be not nore than a few percent of the zero field stress. The incorporation of dislocation widths into the calculation leads to a behavior which is somewhat different, but qualitatively similar to the bcc (zero-width) case. If, however, the assumption of perfect screening is the most valid approach for fcc metals, large oscillations in the stress versus ω_m/ω_c curves are predicted, $\sim$10–30% of the zero-field stress.

Expressions for the electric fields, currents, and charge density associated with a moving dislocation are derived in Sec. V. These are found to have functional forms of the Friedel oscillatory type, similar to those obtained for stationary dislocations,[12,29] but depending critically on the dislocation velocity. It seems likely that experimental observation of the electromagnetic effects of a moving dislocation is possible.

Recently, previous work on this problem has been criticized by Elbaum and Hikata[32] on two counts: (1) experimental results on Pb in the normal state from 4.2 to 15°K show a temperature-independent electron drag coefficient[23]; (2) since most of the energy dissipation is associated with the large $\mathbf{q}(q\gtrsim q_D/10)$ components of the Fourier synthesis, and since phonons for which $q\Lambda\gg1$ have an interaction with electrons which is independent of Λ, the result for the electron-dislocation interaction should be temperature-independent, also. With regard to the first point, it is clear, in view of the new results presented in this paper for fcc metals, that this objection no longer applies. With regard to the second, we remark that there is no particular reason to view the Fourier components of the displacement field as phonons. On the contrary, the scattering processes which electrons may undergo with the dislocation must be such that the Burgers vector and displacement field are conserved. This constraint may be what forces the energy dissipation to occur via the mechanism discussed in this paper, and any proper scattering calculation must take it into account. We hope to make these ideas more concrete in future calculations. At any rate, regardless of the type of theory required for a complete scattering calculation, we feel that the agreement between theory and experiment is sufficiently good to verify the essential correctness of the Boltzmann-equation results.

---

[32] C. Elbaum and A. Hikata, Phys. Rev. Letters **20**, 264 (1968).